An entirely specific type I A-kinase anchoring protein that can sequester two molecules of protein kinase A at mitochondria

Christopher K. Means[a], Birgitte Lygren[b], Lorene K. Langeberg[a], Ankur Jain[c], Rose E. Dixon[d], Amanda L. Vega[d], Matthew G. Gold[a], Susanna Petrosyan[e], Susan S. Taylor[f], Anne N. Murphy[e], Taekjip Ha[c,g], Luis F. Santana[d], Kjetil Tasken[b], and John D. Scott[a,1]

[a]Howard Hughes Medical Institute, Department of Pharmacology, University of Washington School of Medicine, 1959 Pacific Avenue NE, Seattle, WA 98195; [b]Biotechnology Center of Oslo and Center for Molecular Medicine Norway, Nordic European Molecular Biology Laboratory Partnership, University of Oslo, N-0317 Oslo, Norway; [c]Center for Biophysics and Computational Biology, University of Illinois at Urbana-Champaign, Urbana, IL 61822; [d]Department of Physiology and Biophysics, University of Washington, Seattle, WA 98195; [e]Department of Pharmacology, University of California at San Diego, La Jolla, CA 92093; [f]Howard Hughes Medical Institute, Department of Chemistry and Biochemistry, University of California at San Diego, La Jolla, CA 92093; and [g]Howard Hughes Medical Institute, Department of Physics and Center for the Physics of Living Cells, University of Illinois at Urbana-Champaign, Urbana, IL 61822

Edited by* Joseph A. Beavo, University of Washington School of Medicine, Seattle, WA, and approved October 5, 2011 (received for review May 6, 2011)

A-kinase anchoring proteins (AKAPs) tether the cAMP-dependent protein kinase (PKA) to intracellular sites where they preferentially phosphorylate target substrates. Most AKAPs exhibit nanomolar affinity for the regulatory (RII) subunit of the type II PKA holoenzyme, whereas dual-specificity anchoring proteins also bind the type I (RI) regulatory subunit of PKA with 10–100-fold lower affinity. A range of cellular, biochemical, biophysical, and genetic approaches comprehensively establish that sphingosine kinase interacting protein (SKIP) is a truly type I-specific AKAP. Mapping studies located anchoring sites between residues 925–949 and 1,140–1,175 of SKIP that bind RI with dissociation constants of 73 and 774 nM, respectively. Molecular modeling and site-directed mutagenesis approaches identify Phe 929 and Tyr 1,151 as RI-selective binding determinants in each anchoring site. SKIP complexes exist in different states of RI-occupancy as single-molecule pull-down photobleaching experiments show that 41 ± 10% of SKIP sequesters two YFP-RI dimers, whereas 59 ± 10% of the anchoring protein binds a single YFP-RI dimer. Imaging, proteomic analysis, and subcellular fractionation experiments reveal that SKIP is enriched at the inner mitochondrial membrane where it associates with a prominent PKA substrate, the coiled-coil helix protein ChChd3.

Versatile use of gene products is necessary to accomplish all aspects of cellular behavior as the human genome consists of fewer than 25,000 genes. Individual genes may code multiple proteins (1) and temporal patterns of protein synthesis and degradation underlie cell differentiation and organogenesis (2, 3). Posttranslational modification and protein-protein interactions also add to cellular complexity (4). Polymers of actin or tubulin uphold the cytoskeletal architecture whereas assorted structural, modulator, and catalytic proteins assemble sophisticated molecular machines such as the ribosome, proteosomes, or nuclear pore complex (5–7). Although less intricate, hormone responsive G-protein-coupled receptor complexes embedded in the plasma membrane generate chemical messengers that are relayed to intracellular signal transduction cascades (8, 9).

The second messenger cAMP principally activates protein kinase A (PKA) (10, 11). The PKA holoenzyme is a heterotetramer consisting of two regulatory (R) subunits that maintain two catalytic (C) subunits in an inhibited state (12). When cAMP levels are low, the PKA holoenzyme is dormant; however, when cAMP levels are elevated, two molecules bind to each R subunit, thereby releasing the active C subunits. The C subunits phosphorylate serine/threonine residues on target substrates, typically within the sequence context of -R-R-X-S/T-X (13). The prominence of PKA as a mediator of cAMP responsive events is reflected by the prevalence of multiple R and C subunit genes. Two C subunit genes encode the ubiquitously expressed Cα and Cβ isoforms (14). The four R subunit genes are subdivided into two classes: type I [RI (RIα and RIβ)] and type II [RII (RIIα and RIIβ)] (15–17). Although all R subunits share 75% identity in their cAMP binding pockets, the RI and RII classes differ in their sensitivity to cAMP, phosphorylation patterns, and subcellular location (18–20).

Spatial and temporal organization requires a family of noncatalytic modulator proteins called A-kinase anchoring proteins (AKAPs) (21). To date 47 human AKAP genes have been identified that encode proteins which direct PKA to defined intracellular locations (22, 23). The majority of these sequester type II PKA subtypes (24–26), although several dual-function AKAPs can bind either RI or RII (27–29). Here we report that sphingosine kinase interacting protein (SKIP) anchors the type I PKA holoenzyme exclusively. SKIP is enriched at mitochondria where it can simultaneously anchor two type I PKA holoenzymes to phosphorylate another component of this protein assembly, the inner mitochondrial membrane protein ChChd3.

Results

SKIP Interacts with PKA. SKIP was designated a PKA anchoring protein on the basis of homology with other AKAPs and its detection in a mass spectrometry screen for proteins enriched by purification on cAMP affinity resin (30, 31). However, AKAPs are normally defined by their ability to interact directly with PKA (32). To investigate putative PKA anchoring properties, we expressed FLAG epitope-tagged SKIP in HEK293 cells. FLAG immune complexes were assayed for cofractionation of PKA activity using kemptide as a substrate (Fig. 1*A*). FLAG-AKAP79 immune complexes served as a standard and FLAG-Trim63 immune complexes were negative controls. PKA activity was enriched in the SKIP and AKAP79 immune complexes (Fig. 1*A*, columns 1–4). Kinase activity was blocked by the PKA inhibitor peptide (PKI)

Author contributions: C.K.M., B.L., L.K.L., M.G.G., T.H., K.T., and J.D.S. designed research; C.K.M., B.L., L.K.L., A.J., R.E.D., A.L.V., and M.G.G. performed research; A.J., R.E.D., A.L.V., S.P., S.S.T., A.N.M., T.H., and L.F.S. contributed new reagents/analytic tools; C.K.M., B.L., L.K.L., A.J., M.G.G., K.T., and J.D.S. analyzed data; and C.K.M., M.G.G., and J.D.S. wrote the paper.

The authors declare no conflict of interest.

*This Direct Submission article had a prearranged editor.

Freely available online through the PNAS open access option.

[1]To whom correspondence should be addressed. E-mail: scottjdw@u.washington.edu.

See Author Summary on page 19105.

This article contains supporting information online at www.pnas.org/lookup/suppl/doi:10.1073/pnas.1107182108/-/DCSupplemental.

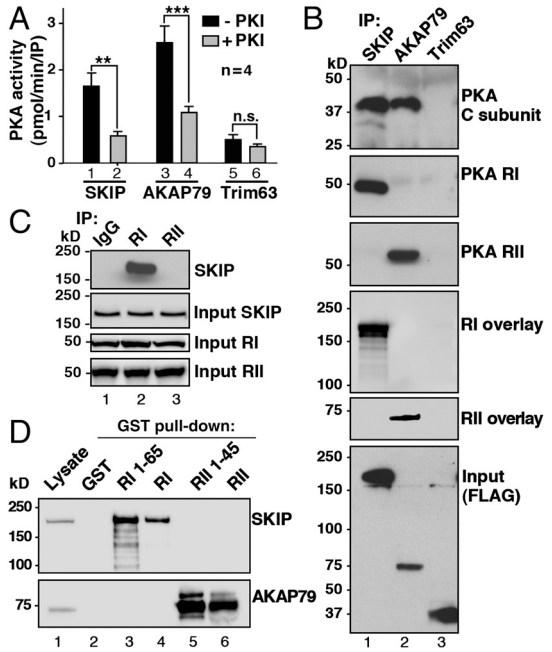

Fig. 1. SKIP is an RI-selective AKAP. (*A*) HEK293 cells were transfected with vectors encoding FLAG-SKIP, FLAG-AKAP79, or FLAG-Trim63. FLAG immune complexes were analyzed for PKA activity in the presence or absence of PKI (means ± SEM, $n = 4$, $^{**}p \leq 0.01$, $^{***}p \leq 0.001$). (*B*) FLAG immune complexes from HEK293 cells were immunoblotted with antibodies against the catalytic (*Top*), RI (*Second*), or RII (*Third*) subunits of PKA, or overlayed with purified labeled RI (*Fourth*) or RII (*Fifth*) protein. Immunoblot of input lysate is shown in *Bottom*. (*C*) Lysates from HEK293 cells expressing SKIP were immunoprecipitated with IgG, RI, or RII antibodies and immunoblotted for SKIP. Input lysate is shown in *Bottom*. (*D*) GST or GST-fused PKA regulatory subunits or fragments (indicated above each lane) were purified on glutathione sepharose. GST pull-downs were blotted for SKIP (*Top*) or AKAP79 (*Bottom*).

(Fig. 1*A*, columns 2 and 4) (33). PKA activity was not detected above background in control immune complexes (Fig. 1*A*, columns 5 and 6).

PKA holoenzyme subtypes are classified on the basis of their RI or RII regulatory subunits (34). A series of experiments examined whether SKIP preferentially associates with RI or RII subunits. First, HEK293 cells were transfected with plasmids encoding FLAG-tagged constructs for SKIP, AKAP79, or Trim63. Immune complexes were isolated with FLAG agarose and copurification of endogenous PKA subunits was detected by Western blotting (Fig. 1*B*). The C subunit copurified with SKIP and AKAP79 (Fig. 1*B*, *Top*, lanes 1 and 2). Only the RI subunit was detected in SKIP immune complexes (Fig. 1*B*, *Second*, lane 1). RII was detected in AKAP79 immune complexes (Fig. 1*B*, *Third*, lane 2) and Trim63 was unable to coprecipitate either R subunit (Fig. 1*B*, lane 3).

Second, direct binding to digoxigenin labeled RI or RII was evaluated by protein overlay. RI overlays only detected SKIP (Fig. 1*B*, *Fourth*, lane 1) whereas RII overlays only detected AKAP79 (Fig. 1*B*, *Fifth*, lane 2). Third, reciprocal experiments detected SKIP by immmunoblot only in endogenous RI immune complexes (Fig. 1*C*, *Top*, lane 2). Fourth, a docking and dimerization (D/D) domain on each R subunit forms a binding interface for AKAPs (20, 35). This domain corresponds to the first 65 amino acids of RI and residues 1–45 of RII (36, 37). GST pull-down assays demonstrated that RI 1–65 is sufficient to interact with SKIP (Fig. 1*D*, *Top*, lanes 3 and 4) and confirmed that the RII 1–45 fragment binds AKAP79 (Fig. 1*D*, *Bottom*). Taken together, these experiments show that SKIP binds selectively and directly to the D/D domain of the type I regulatory subunit of PKA.

SKIP Contains Two RI Binding Sites. Mapping experiments with a family of recombinant fragments of SKIP identified two distinct RI anchoring sites; the first is located between amino acids 900–950 and the second within amino acids 1,140–1,175 (Fig. S1). Cell-based studies that summarize these findings are presented in Fig. 2*A*. FLAG-SKIP or fragments lacking one or both of the RI anchoring regions were immunoprecipitated from HEK293 cell lysates. Each immune complex was probed by immunoblot for copurification of the RI and C subunits of PKA (Fig. 2*A*, *Top* and *Third*). Deletion of the first region (SKIP Δ1) reduced the detection of the type I PKA (Fig. 2*A*, *Top* and *Third*, lane 3); removal of the second anchoring site (SKIP Δ2) markedly reduced detection of type I PKA (Fig. 2*A*, *Top* and *Third*, lane 4); and loss of both PKA anchoring sites (SKIP Δ1,2) abolished all interaction with type I PKA (Fig. 2*A*, *Top* and *Third*, lane 5). Controls verified that equivalent amounts of each protein were expressed (Fig. 2*A*, *Fourth*, *Fifth*, and *Sixth*) and that SKIP or deletion mutants did not interact with RII (Fig. 2*A*, *Second*, lanes 2–5).

PKA activity measurements verified these binding studies (Fig. 2*B*). Kinase activity was detected in SKIP immune complexes (Fig. 2*B*, column 1); copurification of PKA activity decreased by approximately 50% when the SKIP Δ1 fragment was immunoprecipitated (Fig. 2*B*, column 3). Coprecipitation of PKA activity was further reduced when SKIP Δ2 was used as the anchoring protein and only baseline levels of kinase activity were detected when the SKIP double mutant (Δ1,2) was used to capture the kinase (Fig. 2*B*, columns 5 and 7). All PKA activity was blocked by the PKI peptide and background levels of kinase activity were measured in Trim63 immune complexes. Thus, removal of either anchoring site on SKIP impairs interaction with type I PKA and loss of both regions abolishes kinase anchoring. Complementary approaches established that either site 1 or site 2 is sufficient for type I PKA anchoring inside cells (Fig. S2).

Bacterially expressed FLAG-tagged fragments encompassing residues 750–1,100 and residues 1,100–1,400 of SKIP were purified to homogeneity by affinity chromatography (Fig. 2 *C* and *D*). Quantitative biochemical analyses measured the RI binding affinities of each fragment. An AlphaScreen amplified luminescent proximity assay detected a strong interaction when either SKIP fragment (concentration range 2.5–320 nM) was used as the donor and RI (1.25–20 nM) served as the acceptor (Fig. 2 *E* and *F*) (38). Competition experiments using anchoring disruptor peptides revealed that the RI-selective anchoring disruptor peptide was most effective at perturbing the interaction between RI and SKIP fragments (Fig. S3 *A* and *B*). RII (1.25–20 nM) did not bind to either fragment of SKIP (Fig. S3 *C* and *D*). Dissociation constants (K_d) were calculated by surface plasmon resonance to be 73 ± 9 nM ($n = 3$) and 774 ± 160 nM ($n = 3$) for site 1 and site 2, respectively (Fig. 2 *G*–*J*). Collectively, the data in Fig. 2 identify autonomous high affinity RI anchoring sites located between residues 750–1,100 and 1,100–1,400 of SKIP.

RI Binding Determinants and Stoichiometry. Comparison of the anchoring sequences on SKIP to corresponding regions in other AKAPs points toward one striking difference (Fig. 3*A*). An aromatic residue occupies position 4, in each SKIP helix (Phe 929 and Tyr 1,151). Molecular modeling using the coordinates from the D-AKAP2-RI D/D complex (39) suggests that this and neighboring side-chains could interact with the R1 isoform-specificity loop (Fig. 3 *B* and *C*). Support for this concept was provided by site-directed mutagenesis. Initially, substitution of Phe 929 in site 1 with Ala or Tyr 1,151 in site 2 with Ala abolished RI binding in each SKIP fragment (Fig. 3*D*, *Top*, lanes 2 and 4). Likewise, double substitution of Phe 929 and Tyr 1,151 with alanine in the context of the full-length protein had a pronounced effect on the anchoring of endogenous RI (Fig. 3 *E*, *Top*, lane 4 and 3*F*). Loading controls confirmed equivalent expression of each SKIP mu-

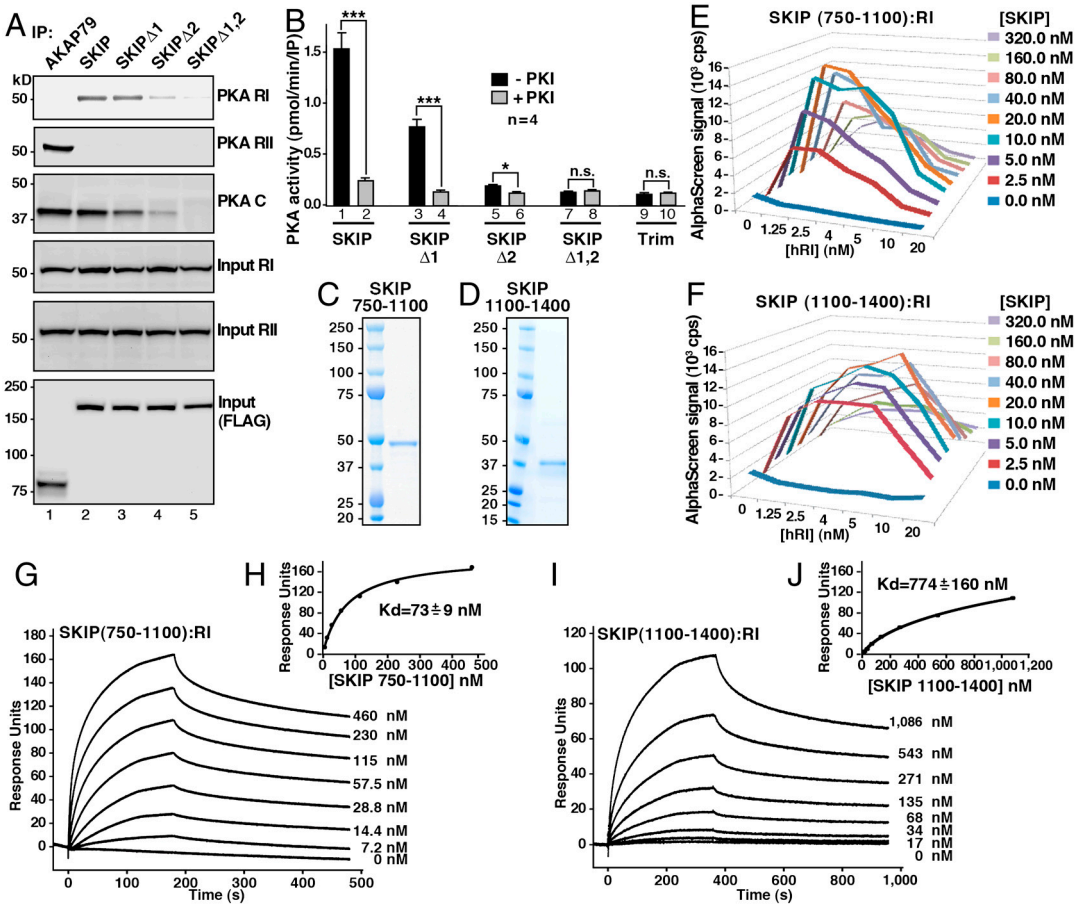

Fig. 2. SKIP contains two independent RI-selective binding sites. (*A*) HEK293 cells were transfected with constructs for FLAG-AKAP79, FLAG-SKIP, or FLAG-SKIP lacking amino acids 900–950 (SKIP Δ1), amino acids 1,140–1,175 (SKIP Δ2), or amino acids 900–950 and 1,140–1,175 (SKIP Δ1,2). FLAG immune complexes were immunoblotted with antibodies against the RI (*Top*), RII (*Second*), or catalytic (*Third*) subunit of PKA. Input lysate is shown in lower three panels. (*B*) HEK293 cells were transfected with SKIP, SKIP Δ1, SKIP Δ2, SKIP Δ1,2, or Trim63. FLAG immune complexes were analyzed for PKA activity in the presence or absence of PKI (means ± SEM, $n = 4$, $*p \leq 0.01$, $***p \leq 0.001$). (*C–D*) Coomassie blue stain of affinity-purified FLAG-SKIP 750–1,100 (*C*) and FLAG-SKIP 1,100–1,400 (*D*). (*E–F*) AlphaScreen assay performed with varying concentrations of purified FLAG-SKIP 750–1,100 (*E*) or FLAG-SKIP 1,100–1,400 (*F*) and biotinylated RI. Cross-titration was performed with anti-FLAG acceptor beads together with streptavidin donor beads. (*G–J*) Surface plasmon resonance analysis of FLAG-SKIP 750–1,100 (*G*) or FLAG-SKIP 1,100–1,400 (*I*) binding to immobilized RI. (*H* and *J*) Steady-state binding curves with dissociation constants (K_d) for interaction between SKIP 750–1,100 (*H*) or SKIP 1,100–1,400 (*J*) and RI. Data is representative of three independent experiments run on different surfaces (means ± SEM, $n = 3$).

tant (Fig. 3 *D* and *E*, *Bottom*). Studies presented as supplemental data show that point mutations that disrupt helicity (proline substitution) abolished RI anchoring in each SKIP fragment and in the context of full-length protein (Fig. S4 *A* and *B*). Collectively these studies argue that the aromatic side-chains which protrude from helices in two regions of SKIP are determinants for RI-selective anchoring. Supplementary modeling studies indicate that the RII D/D does not have the capacity to interface with Phe 929 and Tyr 1,151 (Fig. S4 *C* and *D*).

A logical and testable extension of these findings was to establish whether two RI dimers simultaneously associate with each SKIP molecule. The stoichiometry of the SKIP-RI complexes was evaluated by the single-molecule pull-down (SiMPull) assay (40). FLAG-tagged SKIP and YFP-RI were coexpressed in HEK293 cells. Cells were lysed and SKIP/YFP-RI complexes were immediately captured on a quartz surface coated with anti-FLAG monoclonal antibodies (Fig. 3 *G* and *H*). Chambers coated with anti-GST antibodies or buffer alone served as controls (Fig. 3 *I* and *J*). Total internal reflection detection of YFP fluorescence marked individual immoblized SKIP/RI complexes. The fluorescent signal was enriched in the anti-FLAG coated chambers as compared to the control surfaces (Fig. 3 *H–K*). The number of sequential photobleaching steps required to quench YFP fluorescence at individual spots was used to calculate the number of RI-moieties in complex with each SKIP (Fig. 3*L*). Fluorescence decay time trajectories of 1,699 individual YFP spots were monitored in four separate experiments (Fig. 3*M*). Nearly all (97%) of the YFP spots bleached in four or fewer steps (Table S1), thus indicating the possibility of up to four YFP moieties per SKIP molecule (Fig. 3*N*). The observed distribution from a representative experiment (orange) fits well to the sum of the two binomial distributions (gray), with 59 ± 10% ($n = 4$) of single RI dimer/SKIP complexes and 41 ± 10% ($n = 4$) of two RI dimer/SKIP complexes (Fig. 3*M*). The probability of an individual YFP actively fluorescing was measured to be 70 ± 3% ($n = 4$). Thus SKIP has the capacity to anchor 0, 1, or 2 molecules of RI dimer in situ and may exist in dynamic equilibrium between distinct occupancy states (Fig. 3*N*).

Ablation of the RIα Gene Abolishes SKIP Interaction with PKA. A rigorous genetic test of our hypothesis that SKIP is an exclusive RI anchoring protein was conducted in mouse embryonic fibroblasts (MEF) from RIα −/− mice. These cells do not express RIα and thus are devoid of type I PKA (41). Initially, wild-type MEFs expressing FLAG-SKIP or FLAG-AKAP79 were generated, and FLAG immune complexes were assessed for copurification of PKA subunits by Western blotting and kinase activity (Fig. 4*A*, *Top* and *Middle* and 4*B*). PKA subunits and kinase activity copurified with SKIP and AKAP79 isolated from wild-type MEFs (Fig. 4*B*, columns 1 and 3). However, when SKIP immune com-

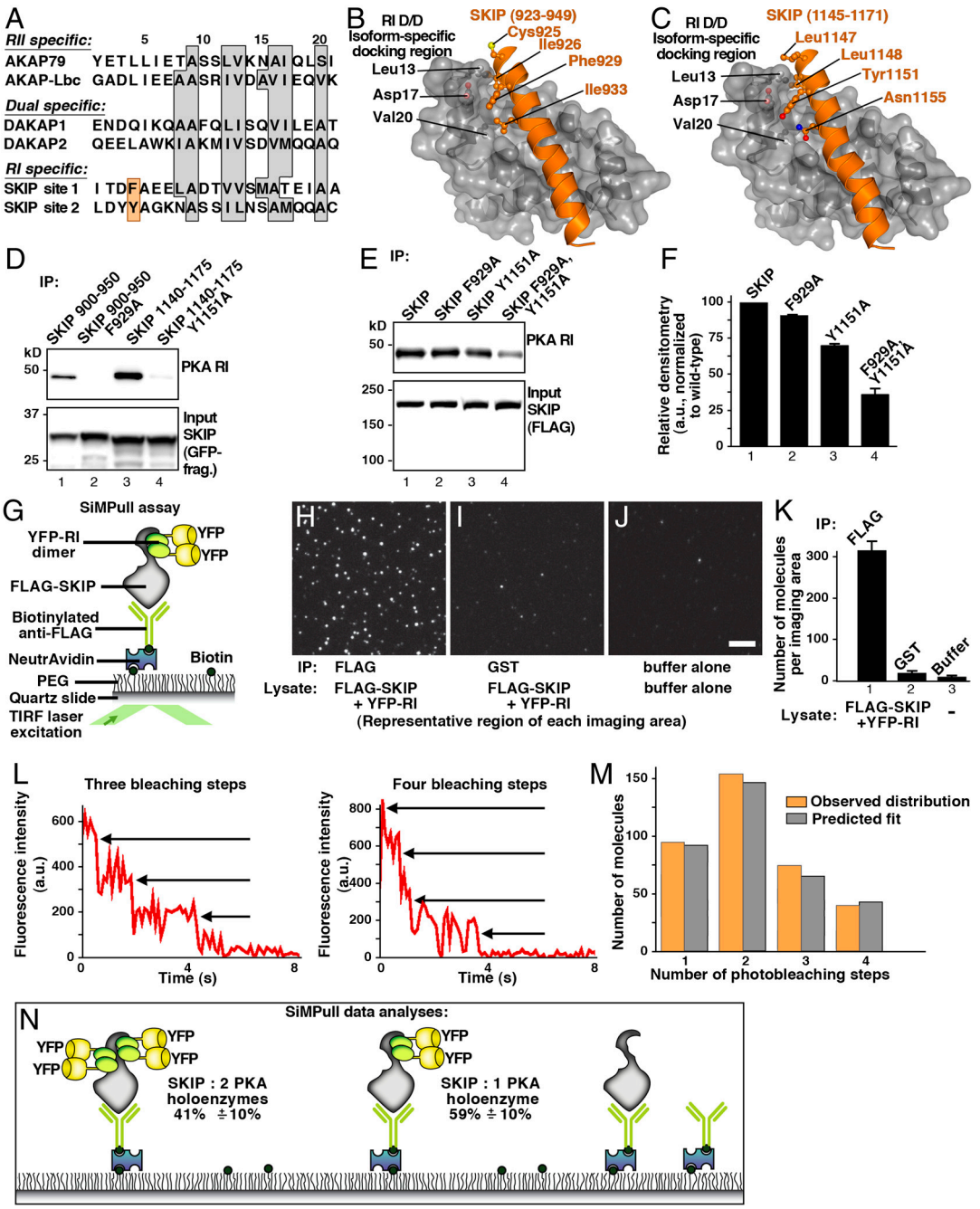

Fig. 3. Stoichiometry and modeling of SKIP-RI interaction. (*A*) Alignment of amphipathic helices from three classes of AKAP protein. Residues are numbered according to the convention of previous structural studies (25, 26). (*B–C*) Structural models of RI (gray). SKIP (orange) interactions are presented following superposition of SKIP residues 923–949 (*B*) and 1,145–1,171 (*C*) onto the equivalent region of D-AKAP2 in the D-AKAP2 PKA RI D/D crystal structure [Protein Data Bank (PDB) ID code 3IM4]. (*D–E*) Alanine substitution of Phe929 and Tyr1151 abolishes RI binding in each GFP-fused binding fragment of SKIP (*D*) and significantly reduces RI binding in the context of full-length FLAG-SKIP (*E*). (*F*) Amalgamated densitometric analysis of RI binding to alanine substitution mutants of full-length FLAG-SKIP. (*G*) Representation of SiMPull assay performed to calculate stoichiometry of SKIP-RI complex. (*H–J*) YFP fluorescence from representative regions of different imaging surfaces. YFP fluorescence from anti-FLAG (*H*) or anti-GST (*I*) coated surface incubated with FLAG-SKIP and YFP-RI lysate or from surface alone not incubated with lysate (*J*). (*K*) Quantitation of YFP molecules on entire imaging surfaces from four independent experiments. (*L*) Representative decay time trajectories of a YFP spot requiring three or four photobleaching steps to quench YFP fluorescence. (*M*) Observed distribution of photobleaching steps from a representative experiment and predicted fit to two binomial distributions. (*N*) Schematic illustrating proportions of SKIP bound to one or two RI dimers as calculated by the SiMPull assay.

plexes were isolated from RIα −/− MEFs stably expressing FLAG-SKIP-GFP, neither regulatory subunits nor PKA activity was detected (Fig. 4*C*, *Top*, lane 1; 4*D*, column 1; and Fig S5). Importantly, reexpression of V5-tagged RIα-mCherry restored SKIP-associated RI and PKA activity (Fig. 4*C*, *Top*, lane 2; 4*D*, column 3; and Fig. S5). These experiments conclusively determine that SKIP does not interact with type II PKA inside cells.

SKIP Directs RI to Mitochondria. The subcellular distribution of SKIP and RI was evaluated by immunofluorescence confocal microscopy. In COS-7 cells, GFP-SKIP exhibited significant overlap with endogenous RI (Fig. 5 *A*, *B*, *E*, and *F*). Furthermore, the subcellular distribution of both proteins was similar and exhibited a pattern reminiscent of mitochondria. Counterstaining with the mitochondrial marker protein Mitofusin-1 or with the MitoTrack-

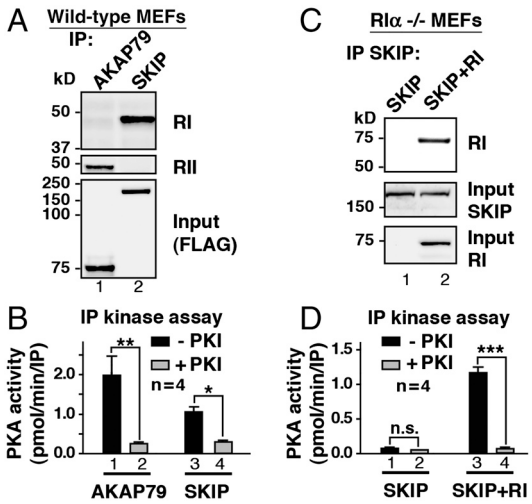

Fig. 4. SKIP anchoring in RIα −/− mouse embryonic fibroblasts. (*A*) Wild-type MEFs transfected with FLAG-AKAP79 or FLAG-SKIP and FLAG immune complexes were immunoblotted with antibodies against RI (*Top*) or RII (*Middle*). Input lysate is shown in *Bottom*. (*B*) FLAG immune complexes were analyzed for PKA activity in the presence or absence of PKI (means ± SEM, $n = 4$, $*p \leq 0.05$, $**p \leq 0.01$). (*C*) RIα −/− MEFs expressing FLAG-SKIP-GFP or both FLAG-SKIP-GFP and V5-RI-mCherry were selected by flow cytometry. FLAG-SKIP immune complexes were immunoblotted with antibodies against RI (*Top*). Input lysate is shown in lower panels. (*D*) PKA activity measurements were performed in the presence or absence of PKI with FLAG immune complexes isolated from RIα −/− MEFs expressing FLAG-SKIP-GFP or FLAG-SKIP-GFP and V5-RI-mCherry (means ± SEM, $n = 4$, $***p \leq 0.001$).

er dye further supported this concept (Fig. 5 *C* and *G*). Moreover, the subcellular location of endogenous RI at mitochondria was more pronounced in cells overexpressing SKIP (Fig. 5 *F* and *H*). Antipeptide antibodies against residues 44–65 of the anchoring protein were generated to detect endogenous SKIP in adult cardiac myocytes where this anchoring protein is enriched (30). Mouse SKIP was detected in two subcellular locations: a striated staining pattern reminiscent of Z bands and a distribution that aligns with mitochondrial marker proteins (Fig. 5 *I–R*). Higher magnification images portray an apparent overlap between a fraction of SKIP and RI (Fig. 5 *M–O*) (Pearson's coefficient $0.186 \pm 0.02, n = 11$). Nearly undetectable overlap was measured in cardiomyocytes stained for SKIP and RII (Pearson's coefficient $0.002 \pm 0.01, n = 9$) (Fig. S6 *A–F*). Separate images depict a partial overlap between SKIP and the mitochondrial marker Mitofusin-1 (Fig. 5 *P–R*) (Pearson's coefficient $0.195 \pm 0.01, n = 15$). Live-cell imaging of SKIP-GFP and MitoTracker in pulsatile adult cardiomyocytes offered additional evidence that some of the anchoring protein is localized at mitochondria (Fig. 5 *S–U*, Movie S1).

SKIP Mediates PKA Phosphorylation of ChChd3. On the basis of our cumulative data, we hypothesized that SKIP targets type I PKA to mitochondria, presumably for a role in the phosphorylation of proteins at this location. Accordingly, an MS screen was initiated for SKIP-binding partners of mitochondrial origin that may also be PKA substrates. FLAG-SKIP immune complexes isolated from HEK293 cells were subjected to trypsin proteolysis and the resulting peptides were identified by MS/MS sequencing (Fig. 6*A*, SKIP). Control experiments were performed in parallel on untransfected HEK293 cells (Fig. 6*A*, empty). Detection of the type I PKA subunits RIα, RIβ, Cα, and Cβ served as internal controls. Importantly, we also show that SKIP copurifies with mitochondrial proteins including ChChd3, ChChd6, SAM50, MTX1, and MTX2, which are members of a mitochondrial macromolecular complex (Fig. 6*A*). One prominent mitochondrial PKA substrate detected in this screen is the coiled-coil helix protein ChChd3, a peripheral component of the intermembrane space that is essential for maintaining cristae integrity (42, 43). This tally's with evidence that SKIP partitions to intermembrane space and matrix subfractions prepared from murine heart mitochondria (Fig. 6*B*, *Top*, lanes 3 and 5).

Several biochemical experiments indicate that SKIP and ChChd3 interact. First, ChChd3 was detected by Western blotting in SKIP immune complexes (Fig. 6*C*, *Top*, lane 2). Second, SKIP was present in ChChd3 immunocomplexes when compared to IgG controls (Fig. 6*D*, *Top*, lane 2). Third, an in vitro transcription/translation system was utilized to determine that SKIP directly interacts with ChChd3 as assessed by immunoblot (Fig. 6*E*, *Top*, lane 2). In contrast, in vitro translated AKAP79 is unable to interact with ChChd3 (Fig. 6*E*, *Top*, lane 1). Fourth, immunofluorescence detection of both proteins revealed overlapping staining patterns in adult mouse ventricular myocytes that also coincided with the subcellular distribution of RI (Fig. 6 *F–I*, Fig. S6 *G–J*).

We next examined whether ChChd3 is phosphorylated by SKIP-anchored PKA. SKIP immune complexes were incubated with cAMP (100 μM) and γ-^{32}P ATP. The phosphorylation pattern of proteins in these complexes was resolved by autoradiography (Fig. 6*J*). A faint band of approximately 25 kDa, corresponding to the mass of ChChd3, was detected upon cAMP stimulation (Fig. 6*J*, *Top*, lane 4). Incorporation of ^{32}P into this band is increased 2.8 ± 0.16-fold ($n = 3$) in SKIP immune complexes isolated from cells coexpressing the anchoring protein and ChChd3 (Fig. 6*J*, *Top*, lane 2). In contrast, less ^{32}P incorporation into this 25 kDa band was detected if a PKA anchoring defective mutant of SKIP (SKIP Δ1,2) served as the anchoring protein (Fig. 6*K*, *Top*, lanes 2 and 5). PKI treatment abolishes all ^{32}P incorporation into ChChd3 (Fig. 6*K*, *Top*, lanes 3 and 6).

Finally, knockdown of ChChd3 in HeLa cells verified that SKIP-anchored PKA phosphorylates endogenous ChChd3. Incubation with cAMP (100 μM) enhanced phosphorylation of the 25 kDa protein in SKIP immune complexes isolated from cells treated with scrambled siRNA (Fig. 6*L*, *Top*, lane 2 and 6*M*). Phosphorylation of this 25 kDa protein was reduced in SKIP complexes isolated from cells treated with ChChd3 siRNA (Fig. 6*L*, *Top*, lane 5 and 6*M*). Suppression of ChChd3 expression and equal loading of proteins is shown by immunoblot (Fig. 6*L*, *Second*, *Third*, and *Fourth*). Amalgamated data from three independent experiments are quantitated in Fig. 6*M*. Thus SKIP-anchored type I PKA mediates phosphorylation of the mitochondrial protein ChChd3.

Discussion

In this study we comprehensively establish that SKIP has the capacity to simultaneously target two type I PKA holoenzymes at mitochondria and coordinate cAMP responsive phosphorylation of the inner membrane protein ChChd3. We present not only quantitative data on the stoichiometry of PKA-AKAP complexes inside cells, but also reveal a unique biological context for this anchoring protein as a mediator of PKA phosphorylation at the inner mitochondrial membrane. We also define aromatic residues that occupy position 4 in each SKIP helix (Phe 929 and Tyr 1,151) as unique RI binding determinants that are not conserved in any naturally occurring RII binding proteins or dual-function anchoring proteins (44, 45). A less informative but crucial element of this study is stringent evidence that SKIP is truly an RI-specific anchoring protein. Perhaps the most definitive proof comes from data presented in Fig. 4*D* showing that SKIP cannot anchor PKA in RIα −/− mouse embryonic fibroblasts (41). This genetic evidence augments cell-based support in Fig. 1 showing that SKIP exclusively cofractionates with type I PKA subunits and biochemical characterization of anchoring sequences with nanomolar affinities for RI in Fig. 2. Resolving the subtype selectivity of this AKAP is important in light of

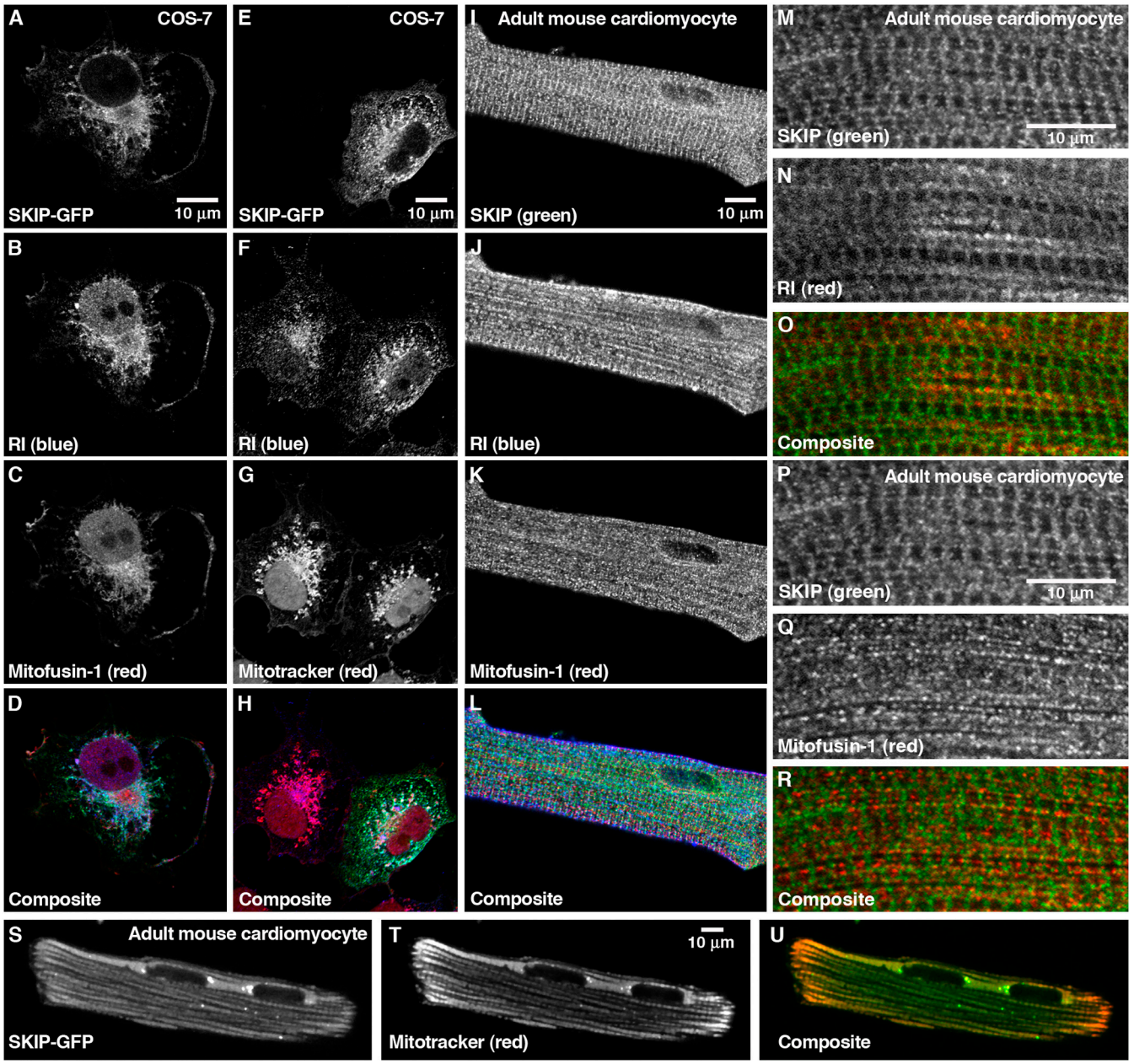

Fig. 5. SKIP and RI localize to mitochondria. (*A–D*) COS-7 cells were transfected with GFP-SKIP (*A*, green), fixed, and then incubated with antibodies against RI (*B*, blue) or Mitofusin-1 (*C*, red). Composite image is shown in *D*. (*E–H*) COS-7 cells expressing GFP-SKIP (*E*, green), were incubated with MitoTracker dye (250 nM) for 30 min prior to fixation (*G*, red), and then incubated with antibodies against RI (*F*, blue). Composite image is shown in *H*. (*I–L*) Adult mouse cardiomyocytes were fixed and incubated with antibodies against SKIP (*I*, green), RI (*J*, blue), and Mitofusin-1 (*K*, red). Composite image is shown in *L*. Higher magnification images of adult mouse cardiomyocytes incubated with antibodies against SKIP (green, *M*, *P*), RI (red, *N*), or Mitofusin-1 (red, *Q*) are shown. Composite images are shown in *O* and *R*. (*S–U*) Images of live GFP-SKIP expressing adult cardiomyocytes loaded with MitoTracker (red).

conflicting reports claiming that SKIP is an RII or RI anchoring protein (30, 45, 46).

SiMPull measurements in Fig. 3 establish that SKIP:2(RI dimer) assemblies form inside cells. This minimally invasive and exquisitely sensitive assay (40) has allowed us to derive two unique fundamental parameters of PKA anchoring. First, nearly 5% of the available YFP-RI associates with SKIP. This distribution was calculated by factoring the total pool of fluorescent RI against the proportion of YFP signal emanating from captured AKAP-RI complexes. At first glance it may seem surprising that such a small proportion of PKA is associated with SKIP. However, this number is likely to reflect the situation in vivo as the concentration of endogenous type I PKA holoenzyme is 3–5 uM (18), a significant proportion of RI is thought to be soluble (19), and other dual-function anchoring proteins compete for YFP-RI (27). Second, the observed and predicted number of photobleaching steps required to quench SKIP-associated fluorescence in Fig. 3*M* infer a mixed population of SKIP:RI dimer and SKIP:2(RI dimer) assemblies, where the anchoring of a single PKA holoenzyme predominates. Several factors could influence this submaximal stoichiometry. For example, both RI binding sites have different affinities for the kinase. The first PKA binding site (residues 925–949) binds RI with a dissociation constant of 73 nM. On the contrary, site 2 (residues 1,140–1,175) binds RI with tenfold lower affinity of 774 nM in vitro. Plausible explanations that reconcile these differences include a loss of cooperativity between both RI anchoring sites upon the analysis of individual SKIP fragments, covalent modifications of the SKIP protein in

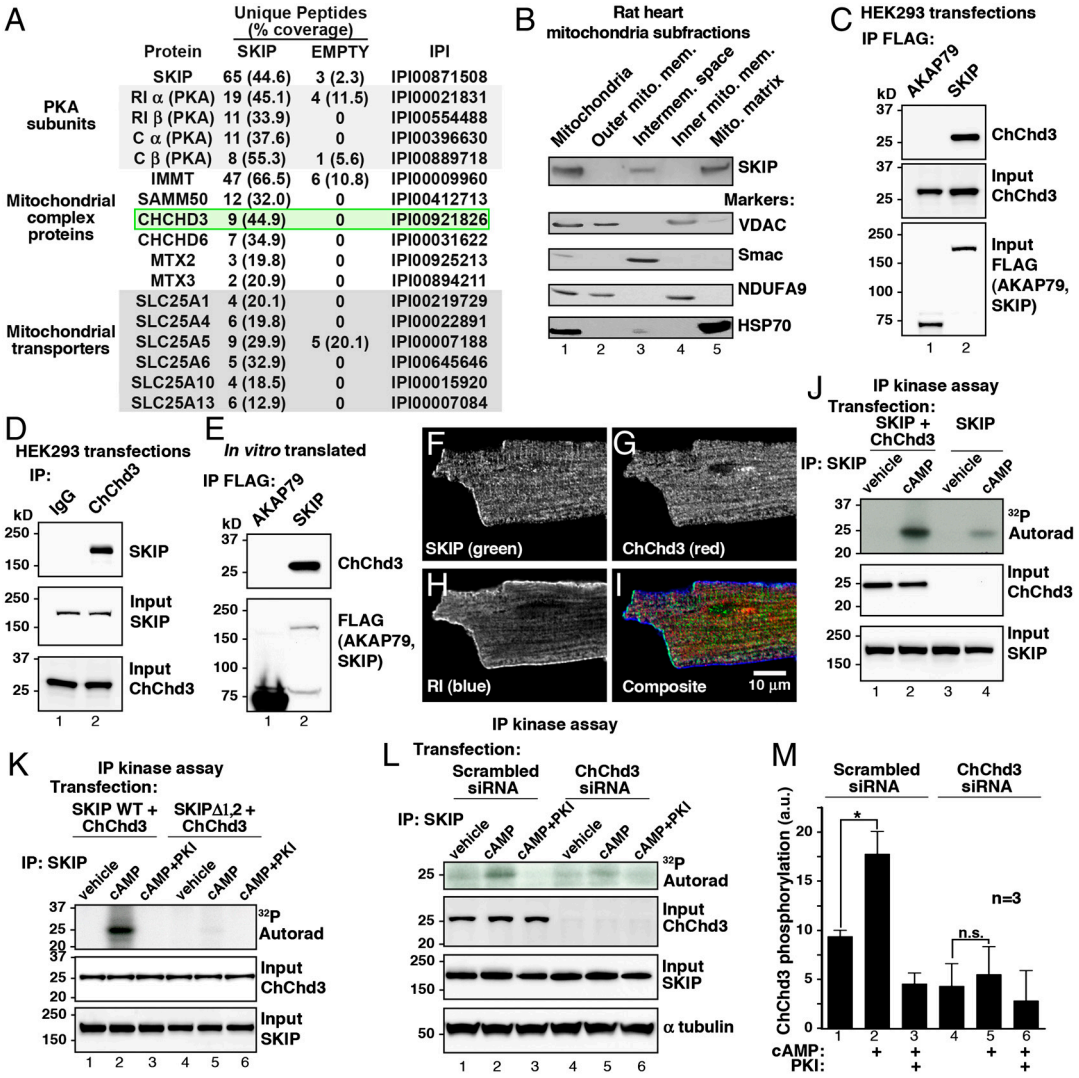

Fig. 6. SKIP associates with and mediates PKA phosphorylation of ChCh3. (*A*) Mass spectrometry screening for mitochondrial SKIP-binding partners. FLAG-SKIP immune complexes isolated from HEK293 cells were proteolyzed and peptides were identified by MS/MS sequencing. Samples from SKIP immune complexes (SKIP) were compared to immune complexes from cells transfected with empty vector (empty). The name of each protein, the number of peptides identified, percent sequence coverage, and IP identification number are indicated above each column. Mitochondrial proteins are indicated. (*B*) Immunoblot detection of SKIP in mitochondrial subfractions. The name of each subfraction is indicated above each lane. Enrichment for the mitochondrial marker proteins VDAC (outer mitochondrial membranes), Smac (intermembrane space), NDUF A9 (inner mitochondrial membrane), and HSP70 (matrix) was used to assess quality of subfractionation. (*C*) HEK293 cells were transfected with V5-ChCh3 and either FLAG-AKAP79 or FLAG-SKIP. FLAG immune complexes were immunoblotted for V5-ChCh3 (*Top*). Input lysate is shown in *Middle* and *Bottom*. (*D*) V5-ChCh3 immune complexes were isolated and immunoblotted for FLAG-SKIP. Input lysate is shown in *Middle* and *Bottom*. (*E*) In vitro-translated V5-ChCh3 was incubated with in vitro-translated FLAG-SKIP or FLAG-AKAP79. FLAG immune complexes were immunoblotted for ChCh3 (*Top*). Input lysate is shown in *Bottom*. (*F–I*) Immunofluorescence images of adult mouse cardiomyocytes incubated with antibodies against SKIP (*F*, green), ChCh3 (*G*, red), and RI (*H*, blue). The composite image is shown in *I*. (*J–M*) Phosphorylation of ChCh3 by SKIP-anchored PKA. (*J*) HEK293 cells were transfected with FLAG-SKIP or FLAG-SKIP and V5-ChCh3. FLAG immune complexes were treated with vehicle or cAMP (100 μM) in the presence of γ-^{32}P ATP. Phosphoproteins were resolved by SDS-PAGE and detected by autoradiography (*Top*). Input lysate is shown in *Middle* and *Bottom*. (*K*) HEK293 cells were cotransfected with V5-ChCh3 and either FLAG-SKIP or FLAG-SKIPΔ1,2. FLAG immune complexes were isolated and stimulated with vehicle, cAMP (100 μM), or cAMP and PKI, in the presence of γ-^{32}P ATP. Phosphoproteins were resolved by SDS-PAGE and detected by autoradiography (*Top*). Input lysate is shown in *Middle* and *Bottom*. (*L*) HeLa cells were transfected with FLAG-SKIP and scrambled siRNA or siRNA against ChCh3. FLAG immune complexes were isolated and treated with vehicle, cAMP (100 μM), or cAMP and PKI in the presence of γ-^{32}P ATP. Phosphoproteins were resolved by SDS-PAGE and detected by autoradiography (*Top*). Suppression of ChCh3 expression was assessed by immunoblot (*Second*). Input lysate and loading control are shown in *Third* and *Bottom*. (*M*) Amalgamated densitometric analysis of phosphate incorporation into ChCh3 in FLAG immune complexes isolated from HeLa cells expressing FLAG-SKIP (means ± SEM, $n = 3$, $^*p \leq 0.05$).

situ that could affect comparative RI binding affinity, or the influence of other regions in the native anchoring protein that may enhance or repress PKA binding. Precedent for the latter mechanism is provided by studies on Ezrin that define regions distal to the anchoring site that repress association with PKA (47).

Nevertheless, our findings place SKIP in a select group of anchoring proteins that sequester two PKA holoenzymes. Although AKAP220, Big2, and AKAP450/yotiao have been projected to contain additional RII binding sites (48–50), there is scant experimental evidence to substantiate this conjecture. In this report our combined biochemical, analytical, and single-molecule fluorescence approaches clearly establish that two units of type I PKA holoenzyme can be accommodated per SKIP protomer. A variation on this theme, as recently exemplified by AKAP79/150, is dimerization of anchoring proteins as a means to increase the local concentration of type II PKA (51). Irrespective of which

molecular mechanism is utilized, such multimeric assemblies create a microenvironment surrounding the AKAPs where PKA phosphorylation can be appreciably elevated. These elevated levels of anchored PKA may have particular relevance for the duration of second messenger responses in the vicinity of SKIP because the type I PKA holoenzyme is activated by lower concentrations of cAMP than the type II subtype (52).

SKIP was initially identified as a negative regulator of sphingosine kinase 1 (30). This enzyme is responsible for generation of sphingosine-1-phosphate (S1P), a cardioprotective and antiapoptotic lysophospholipid produced in response to hypoxia and acute ischemia/reperfusion injury (53). PKC and ERKs are known modulators of sphingosine kinase 1 but there is scant evidence of a role for PKA (54–56). Thus, the PKA anchoring and sphingosine kinase 1 binding may represent independent aspects of SKIP function that reside within the same polypeptide chain. This concept is reminiscent of how other cardiac PKA anchoring proteins such as AKAP-Lbc and PI3 kinase γ seem to operate as they also encode catalytic units for guanine nucleotide exchange and lipid kinase activity, respectively (57, 58). Alternatively, our MS evidence that SKIP is recruited into higher order macromolecular complexes within the mitochondrial intermembrane space could enhance PKA phosphorylation of ChChd3 (43) and accommodate an antiapoptotic role for sphingosine kinase 1 (53). It remains to be determined if other SKIP-binding partners organize distinct signaling events at the Z bands of cardiomyocytes where a significant fraction of this anchoring protein also resides.

Materials and Methods

More details of the techniques below are included as *SI Materials and Methods*.

Antibodies. Antibodies for FLAG and FLAG agarose (Sigma), V5 (Invitrogen), RI (BD), RII (BD), PKA catalytic subunit (BD), Mitofusin-1 (Abcam), MitoTracker (Invitrogen), and ChChd3 (Abcam). SKIP antibodies were produced in rabbits by immunizing against peptides from amino acids 44–65 or 1,635–1,649 of SKIP sequence (Covance). Serum was affinity purified against these peptide sequences.

Plasmids and siRNA. SKIP or SKIP truncations were cloned into pcDNA3 (Invitrogen) with N-terminal FLAG epitope or into pEGFP-N3 (Clontech) with C-terminal GFP epitope. AKAP79 and Trim63 were cloned into pcDNA3 with N-terminal FLAG epitopes. ChChd3 was cloned into pcDNA3.1 in frame with V5 epitope. Mutations were created by site-directed mutagenesis with QuikChange Lightning Kit (Stratagene). ChChd3 siRNA was purchased from Thermo. For bacterial expression, RI and RII fragments were cloned into pGEX 6P-1 and SKIP fragments were cloned into pET101. For retrovirus generation, FLAG-GFP-SKIP was cloned into pFB (Stratagene) and V5-RI was cloned into pRetroQ-mCherry (Clontech).

Immunoprecipitation and PKA Activity, Pull-Down Assays, and R Subunit Overlays. Performed as described previously (59). Stoichiometry of SKIP:RI complex was assessed using SiMPull assay (40). Cell staining was as published previously (60). Myocytes were isolated by enzymatic digestion using retrograde aortic perfusion as described previously (61). Mitochondrial fractions were isolated from rat heart as described previously (43).

Mass Spectrometry Analysis. All proteins were subjected to trypsin digestion and peptides were identified by MS/MS sequencing on LTQ Orbitrap instrument as described previously (51).

In Vitro Translation Direct Binding Assay. FLAG-SKIP or FLAG-AKAP79 proteins were synthesized using in vitro translation (Pierce). V5-ChChd3 protein was synthesized by in vitro translation (Promega). Lysates for appropriate proteins were mixed with FLAG agarose and immunoprecipitation was performed as described above.

Statistical Analyses. Analyses were performed using GraphPad Prism. All data are expressed as mean ± SEM. Differences in quantitative variables were examined by one-way analysis of variance (ANOVA) or paired Student's *t* test. A P value of <0.05 was considered significant (*), a P value of <0.01 was considered very significant (**), and a P value of <0.001 was considered extremely significant (***).

ACKNOWLEDGMENTS. The authors wish to thank Dr. Dinesh Hirenallur-Shanthappa for preparation of adult mouse ventricular myocytes, Dr. Elisabeth Jarnaess for input in the early stages of the work, and members of the Scott and Tasken labs for their critical evaluation of this manuscript. This work was supported by DK54441 (to J.D.S, A.N.M., S.S.T.), Fondation Leducq International Network Grant 06CDV02 (to J.D.S.), Research Council of Norway (K.T.), AI083025 and 0822613 (to T.H.), and American Heart Association Grant 0840049N and HL085686 (to L.F.S.). C.K.M. is funded by National Institutes of Health Experimental Pathology of Cardiovascular Disease training Grant T32 HL 07312. M.G.G. is a Sir Henry Wellcome Postdoctoral Research Fellow.

1. Keren H, Lev-Maor G, Ast G (2010) Alternative splicing and evolution: Diversification, exon definition and function. *Nat Rev Genet* 11:345–355.
2. Hunter T (1995) Protein kinases and phosphatases: The yin and yang of protein phosphorylation and signaling. *Cell* 80:225–236.
3. Manning G, Whyte DB, Martinez R, Hunter T, Sudarsanam S (2002) The protein kinase complement of the human genome. *Science* 298:1912–1934.
4. Scott JD, Pawson T (2009) Cell signaling in space and time: Where proteins come together and when they're apart. *Science* 326:1220–1224.
5. Mitchison T, Kirschner M (1984) Dynamic instability of microtubule growth. *Nature* 312:237–242.
6. Hall A (1998) Rho GTPases and the actin cytoskeleton. *Science* 279:509–514.
7. Robinson CV, Sali A, Baumeister W (2007) The molecular sociology of the cell. *Nature* 450:973–982.
8. Lefkowitz RJ (2003) A magnificent time with the "magnificent seven" transmembrane spanning receptors. *Circ Res* 92:342–344.
9. Shcherbakova OG, et al. (2007) Organization of beta-adrenoceptor signaling compartments by sympathetic innervation of cardiac myocytes. *J Cell Biol* 176:521–533.
10. Beavo JA, Brunton LL (2002) Cyclic nucleotide research—still expanding after half a century. *Nat Rev Mol Cell Biol* 3:710–718.
11. Taylor SS, et al. (2004) PKA: A portrait of protein kinase dynamics. *Biochim Biophys Acta* 1697:259–269.
12. Beavo JA, Bechtel PJ, Krebs EG (1974) Preparation of homogenous cyclic AMP-dependent protein kinase(s) and its subunits from rabbit skeletal muscle. *Methods Enzymol* 38:299–308.
13. Kemp BE, Graves DJ, Benjamini E, Krebs EG (1977) Role of multiple basic residues in determining the substrate specificity of cyclic AMP-dependent protein kinase. *J Biol Chem* 252:4888–4894.
14. Brandon EP, Idzerda RL, McKnight GS (1997) PKA isoforms, neural pathways, and behavior: Making the connection. *Curr Opin Neurobiol* 7:397–403.
15. Lee DC, Carmichael DF, Krebs EG, McKnight GS (1983) Isolation of cDNA clone for the type I regulatory subunit of bovine cAMP-dependent protein kinase. *Proc Natl Acad Sci USA* 80:3608–3612.
16. Jahnsen T, et al. (1986) Molecular cloning, cDNA structure, and regulation of the regulatory subunit of type II cAMP-dependent protein kinase from rat ovarian granulosa cells. *J Biol Chem* 261:12352–12361.
17. Scott JD, et al. (1987) The molecular cloning of a type II regulatory subunit of the cAMP-dependent protein kinase from rat skeletal muscle and mouse brain. *Proc Natl Acad Sci USA* 84:5192–5196.
18. Corbin JD, Keely SL, Park CR (1975) The distribution and dissociation of cyclic adenosine 3′:5′-monophosphate-dependent protein kinase in adipose, cardiac, and other tissues. *J Biol Chem* 250:218–225.
19. Corbin JD, Sugden PH, Lincoln TM, Keely SL (1977) Compartmentalization of adenosine 3′,5′-monophosphate and adenosine 3′,5′-monophosphate-dependent protein kinase in heart tissue. *J Biol Chem* 252:3854–3861.
20. Scott JD, et al. (1990) Type II regulatory subunit dimerization determines the subcellular localization of the cAMP-dependent protein kinase. *J Biol Chem* 265:21561–21566.
21. Wong W, Scott JD (2004) AKAP Signalling complexes: Focal points in space and time. *Nat Rev Mol Cell Biol* 5:959–971.
22. Pidoux G, Tasken K (2010) Specificity and spatial dynamics of protein kinase A signaling organized by A-kinase-anchoring proteins. *J Mol Endocrinol* 44:271–284.
23. Welch EJ, Jones BW, Scott JD (2010) Networking with AKAPs: Context-dependent regulation of anchored enzymes. *Mol Interventions* 10:86–97.
24. Carr DW, et al. (1991) Interaction of the regulatory subunit (RII) of cAMP-dependent protein kinase with RII-anchoring proteins occurs through an amphipathic helix binding motif. *J Biol Chem* 266:14188–14192.
25. Gold MG, et al. (2006) Molecular basis of AKAP specificity for PKA regulatory subunits. *Mol Cell* 24:383–395.
26. Kinderman FS, et al. (2006) A dynamic mechanism for AKAP binding to RII isoforms of cAMP-dependent protein kinase. *Mol Cell* 24:397–408.
27. Huang LJ, Durick K, Weiner JA, Chun J, Taylor SS (1997) Identification of a novel dual specificity protein kinase A anchoring protein, D-AKAP1. *J Biol Chem* 272:8057–8064.
28. Huang LJ, Durick K, Weiner JA, Chun J, Taylor SS (1997) D-AKAP2, a novel protein kinase A anchoring protein with a putative RGS domain. *Proc Natl Acad Sci USA* 94:11184–11189.

29. Jarnaess E, et al. (2008) Dual specificity A-kinase anchoring proteins (AKAPs) contain an additional binding region that enhances targeting of protein kinase A type I. *J Biol Chem* 283:33708–33718.
30. Lacana E, Maceyka M, Milstien S, Spiegel S (2002) Cloning and characterization of a protein kinase A anchoring protein (AKAP)-related protein that interacts with and regulates sphingosine kinase 1 activity. *J Biol Chem* 277:32947–32953.
31. Scholten A, et al. (2006) Analysis of the cGMP/cAMP interactome using a chemical proteomics approach in mammalian heart tissue validates sphingosine kinase type 1-interacting protein as a genuine and highly abundant AKAP. *J Proteome Res* 5:1435–1447.
32. Colledge M, Scott JD (1999) AKAPs: From structure to function. *Trends Cell Biol* 9:216–221.
33. Scott JD, Glaccum MB, Fischer EH, Krebs EG (1986) Primary-structure requirements for inhibition by the heat-stable inhibitor of the cAMP-dependent protein kinase. *Proc Natl Acad Sci USA* 83:1613–1616.
34. Scott JD (1991) Cyclic nucleotide-dependent protein kinases. *Pharmacol Ther* 50:123–145.
35. Banky P, et al. (2000) Isoform-specific differences between the type Ialpha and IIalpha cyclic AMP-dependent protein kinase anchoring domains revealed by solution NMR. *J Biol Chem* 275:35146–35152.
36. Newlon MG, et al. (2001) A novel mechanism of PKA anchoring revealed by solution structures of anchoring complexes. *EMBO J* 20:1651–1662.
37. Banky P, et al. (2003) Related protein-protein interaction modules present drastically different surface topographies despite a conserved helical platform. *J Mol Biol* 330:1117–1129.
38. Stokka AJ, et al. (2006) Characterization of A-kinase-anchoring disruptors using a solution-based assay. *Biochem J* 400:493–499.
39. Sarma GN, et al. (2010) Structure of D-AKAP2:PKA RI complex: Insights into AKAP specificity and selectivity. *Structure* 18:155–166.
40. Jain A, et al. (2011) Probing cellular protein complexes using single-molecule pull-down. *Nature* 473:484–488.
41. Amieux PS, et al. (2002) Increased basal cAMP-dependent protein kinase activity inhibits the formation of mesoderm-derived structures in the developing mouse embryo. *J Biol Chem* 277:27294–27304.
42. Schauble S, et al. (2007) Identification of ChChd3 as a novel substrate of the cAMP-dependent protein kinase (PKA) using an analog-sensitive catalytic subunit. *J Biol Chem* 282:14952–14959.
43. Darshi M, et al. (2010) ChChd3, an inner mitochondrial membrane protein, is essential for maintaining crista integrity and mitochondrial function. *J Biol Chem* 286:2918–2932.
44. Alto NM, et al. (2003) Bioinformatic design of A-kinase anchoring protein-in silico: A potent and selective peptide antagonist of type II protein kinase A anchoring. *Proc Natl Acad Sci USA* 100:4445–4450.
45. McLaughlin WA, Hou T, Taylor SS, Wang W (2010) The identification of novel cyclic AMP-dependent protein kinase anchoring proteins using bioinformatic filters and peptide arrays. *Protein Eng Des Sel* 24:333–339.
46. Kovanich D, et al. (2010) Sphingosine kinase interacting protein is an A-kinase anchoring protein specific for type I cAMP-dependent protein kinase. *ChemBioChem* 11:963–971.
47. Ruppelt A, et al. (2007) Inhibition of T cell activation by cyclic adenosine 5′-monophosphate requires lipid raft targeting of protein kinase A type I by the A-kinase anchoring protein ezrin. *J Immunol* 179:5159–5168.
48. Witczak O, et al. (1999) Cloning and characterization of a cDNA encoding an A-kinase anchoring protein located in the centrosome, AKAP450. *EMBO J* 18:1858–1868.
49. Reinton N, et al. (2000) Localization of a novel human A-kinase-anchoring protein, hAKAP220, during spermatogenesis. *Dev Biol* 223:194–204.
50. Li H, Adamik R, Pacheco-Rodriguez G, Moss J, Vaughan M (2003) Protein kinase A-anchoring (AKAP) domains in brefeldin A-inhibited guanine nucleotide-exchange protein 2 (BIG2). *Proc Natl Acad Sci USA* 100:1627–1632.
51. Gold MG, et al. (2011) Architecture and dynamics of an A-kinase anchoring protein 79 (AKAP79) signaling complex. *Proc Natl Acad Sci USA* 108:6426–6431.
52. Otten AD, Parenteau LA, Doskeland S, McKnight GS (1991) Hormonal activation of gene transcription in ras-transformed NIH3T3 cells overexpressing RIIa and RIIb subunits of the cAMP-dependent protein kinase. *J Biol Chem* 266:23074–23082.
53. Means CK, et al. (2007) Sphingosine 1-phosphate S1P2 and S1P3 receptor-mediated Akt activation protects against in vivo myocardial ischemia-reperfusion injury. *Am J Physiol Heart Circ Physiol* 292:H2944–H2951.
54. Johnson KR, Becker KP, Facchinetti MM, Hannun YA, Obeid LM (2002) PKC-dependent activation of sphingosine kinase 1 and translocation to the plasma membrane: Extracellular release of sphingosine-1-phosphate induced by phorbol 12-myristate 13-acetate (PMA). *J Biol Chem* 277:35257–35262.
55. Pitson SM, et al. (2003) Activation of sphingosine kinase 1 by ERK1/2-mediated phosphorylation. *EMBO J* 22:5491–5500.
56. Ma Y, et al. (2005) Sphingosine activates protein kinase A type II by a novel cAMP-independent mechanism. *J Biol Chem* 280:26011–26017.
57. Diviani D, Soderling J, Scott JD (2001) AKAP-Lbc anchors protein kinase A and nucleates Galpha 12-selective Rho-mediated stress fiber formation. *J Biol Chem* 276:44247–44257.
58. Perino A, et al. (2011) Integrating cardiac PIP(3) and cAMP signaling through a PKA anchoring function of p110gamma. *Mol Cell* 42:84–95.
59. Corbin JD, Reimann EM (1974) A filter assay for determining protein kinase activity. *Methods Enzymol* 38:287–294.
60. Dou Y, et al. (2010) Normal targeting of a tagged Kv1.5 channel acutely transfected into fresh adult cardiac myocytes by a biolistic method. *Am J Physiol Cell Physiol* 298:C1343–C1352.
61. Means CK, Miyamoto S, Chun J, Brown JH (2008) S1P1 receptor localization confers selectivity for Gi-mediated cAMP and contractile responses. *J Biol Chem* 283:11954–11963.